

# Defect Annihilation and Proliferation in Active Nematics

Luca Giomi,<sup>1</sup> Mark J. Bowick,<sup>2,3</sup> Xu Ma,<sup>2</sup> and M. Cristina Marchetti<sup>2,3</sup>

<sup>1</sup>*SISSA, International School for Advanced Studies, Via Bonomea 265, 34136 Trieste, Italy*

<sup>2</sup>*Physics Department, Syracuse University, Syracuse NY 13244, USA*

<sup>3</sup>*Syracuse Biomaterials Institute, Syracuse University, Syracuse NY 13244, USA*

Liquid crystals inevitably possess topological defect excitations generated through boundary conditions, through applied fields, or in quenches to the ordered phase. In equilibrium, pairs of defects coarsen and annihilate as the uniform ground state is approached. Here we show that defects in active liquid crystals exhibit profoundly different behavior, depending on the degree of activity and its contractile or extensile character. While contractile systems enhance the annihilation dynamics of passive systems, extensile systems act to drive defects apart so that they swarm around in the manner of topologically well-characterized self-propelled particles. We develop a simple analytical model for the defect dynamics which reproduces the key features of both the numerical solutions and recent experiments on microtubule-kinesin assemblies.

Active liquid crystals are nonequilibrium fluids composed of internally driven elongated units. The key feature that distinguishes them from their well-studied passive counterparts is that they are maintained out of equilibrium not by an external force applied at the system's boundary, such as an imposed shear, but by an energy input on each individual unit. Examples include mixtures of cytoskeletal filaments and associated motor proteins, bacterial suspensions, the cell cytoskeleton, and even nonliving analogues, such as monolayers of vibrated granular rods [1]. The internal drive that characterizes active liquid crystals dramatically changes the system's dynamics and yields novel effects arising from the interplay of orientational order and flow, such as spontaneous laminar flow [2–4], large density fluctuations [5–7], unusual rheological properties [8–10], excitability [11, 12] and low Reynolds number turbulence [12, 13].

Ordered liquid crystalline phases of active matter, like their equilibrium counterparts, exhibit distinctive inhomogeneous configurations known as topological defects. In equilibrium, defect configurations may be generated through boundary conditions, externally applied fields, or rapid quenches to the ordered state. When the constraints are removed or the system is given time to equilibrate, the defects ultimately annihilate [14]. Experiments have shown that in active systems, in contrast, defect configurations can occur spontaneously in bulk and be continuously regenerated by the local energy input [15, 16]. The nature of the topological defects is, of course, intimately related to the symmetry of the system, which can be either polar (like in ferromagnets) or nematic. While the nature of the charge  $+1$  defects that occur in polar active systems has been studied for some time [17–20], the properties of defects in apolar or nematic active media are still largely unexplored. In these systems the defects are charge  $\pm 1/2$  disclinations [21]. Such defects have been identified in monolayers of vibrated granular rods [7] and also in active nematic gels assembled *in vitro* from microtubules and kinesins. In the latter case the defects were shown to drive spontaneous

flows in bulk [16, 22]. When confined at an oil-water interface, furthermore, the gel forms a two-dimensional active nematic film, with self-sustained flows resembling cytoplasmic streaming and the continuous creation and annihilation of defect pairs [16].

In this Letter, we examine the effect of activity on the dynamics of disclinations in a two-dimensional nematic liquid crystalline film [23]. Hydrodynamics plays an important role in controlling the dynamics of defects in liquid crystals. As the defect moves, the coupling between the orientational order parameter and the flow velocity of the fluid yields what is usually called the *backflow* which significantly modifies defect dynamics [24–28]. Here we show that active stresses dramatically affect the defect dynamics by altering the backflow in such a way as to speed up, slow down, or even suppress pair annihilation, according to the extent of activity and the typical time scale of orientational relaxation of the nematic phase. Moreover, when the latter is very large compared to the time scale associated with activity, relaxation is overwhelmed entirely, leading to defect proliferation.

The hydrodynamic equations of active nematic liquid crystals can be obtained from that of passive nematics by the addition of nonequilibrium stresses and currents due to activity [1, 11, 12]. These equations are formulated in terms of a concentration  $c$ , a flow velocity  $\mathbf{v}$  and the nematic tensor order parameter  $Q_{ij} = S(n_i n_j - \frac{1}{2}\delta_{ij})$ , with  $\mathbf{n}$  the director field. The alignment tensor  $Q_{ij}$  is traceless and symmetric, and, hence, has only two independent components in two dimensions. Considering for simplicity the case of an incompressible fluid of constant density  $\rho$ , where  $\nabla \cdot \mathbf{v} = 0$ , the equations are given by

$$\frac{Dc}{Dt} = \partial_i [D_{ij}\partial_j c + \alpha_1 c^2 \partial_j Q_{ij}] , \quad (1a)$$

$$\rho \frac{Dv_i}{Dt} = \eta \nabla^2 v_i - \partial_i p + \partial_j \sigma_{ij} , \quad (1b)$$

$$\frac{DQ_{ij}}{Dt} = \lambda S u_{ij} + Q_{ik} \omega_{kj} - \omega_{ik} Q_{kj} + \gamma^{-1} H_{ij} , \quad (1c)$$

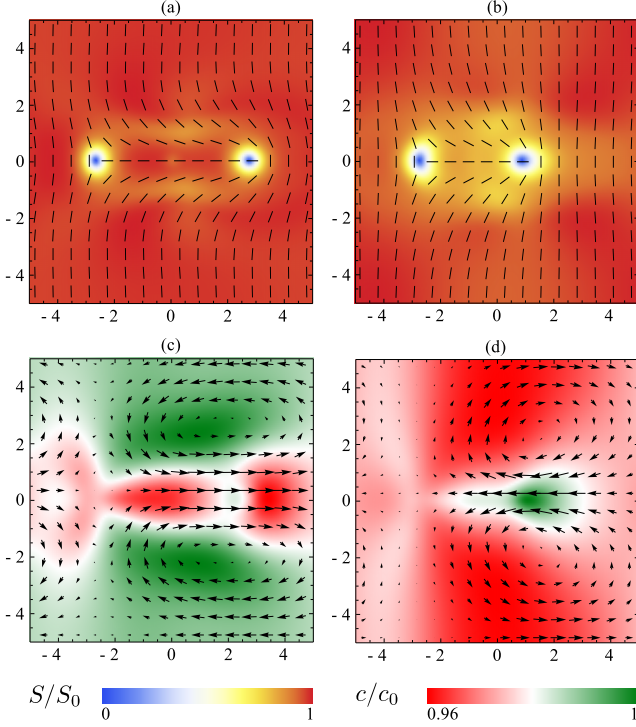


FIG. 1: (color online) Snapshots of a disclination pair shortly after the beginning of relaxation. (Top) Director field (black lines) superimposed on a heat map of the nematic order parameter and (bottom) flow field (arrows) superimposed on a heat map of the concentration for an extensile system with  $\alpha = -0.2$  (a),(c) and a contractile system with  $\alpha = 0.2$  (b),(d). In the top images, the color denotes the magnitude of the nematic order parameter  $S$  relative to its equilibrium value  $S_0 = \sqrt{1 - c^*/c_0}$ . In the bottom images, the color denotes the magnitude of the concentration  $c$  relative to the average value  $c_0$ . Depending on the sign of  $\alpha$ , the backflow tends to speed up ( $\alpha > 0$ ) or slow down ( $\alpha < 0$ ) the annihilation process by increasing or decreasing the velocity of the  $+1/2$  disclination. For  $\alpha$  negative and sufficiently large in magnitude, the  $+1/2$  defect reverses its direction of motion (c) and escapes annihilation.

where  $\frac{D}{Dt} = \partial_t + \mathbf{v} \cdot \nabla$  indicates the material derivative,  $D_{ij} = D_0 \delta_{ij} + D_1 Q_{ij}$  is the anisotropic diffusion tensor,  $\eta$  is the viscosity,  $p$  is the pressure, and  $\lambda$  is the nematic alignment parameter. Here  $u_{ij} = (\partial_i v_j + \partial_j v_i)/2$  and  $\omega_{ij} = (\partial_i v_j - \partial_j v_i)/2$  are the symmetrized rate of strain tensor and the vorticity, respectively. The molecular field  $H_{ij}$  embodies the relaxational dynamics of the nematic phase (with  $\gamma$  a rotational viscosity) and can be obtained from the variation of the Landau-De Gennes free energy of a two-dimensional nematic [21],  $H_{ij} = -\delta F / \delta Q_{ij}$ , with

$$F/K = \int dA \left[ \frac{1}{4}(c - c^*) \text{tr} \mathbf{Q}^2 + \frac{1}{4}c(\text{tr} \mathbf{Q}^2)^2 + \frac{1}{2}|\nabla \mathbf{Q}|^2 \right], \quad (2)$$

where  $K$  is an elastic constant with dimensions of energy,  $\text{tr} \mathbf{Q}^2 = S^2/2$  and  $c^*$  is the critical concentration for the isotropic-nematic transition, so that, at equilibrium,

$S = \sqrt{1 - c^*/c}$ . Finally, the stress tensor  $\sigma_{ij} = \sigma_{ij}^r + \sigma_{ij}^a$  is the sum of the elastic stress due to nematic elasticity,  $\sigma_{ij}^r = -\lambda S H_{ij} + Q_{ik} H_{kj} - H_{ik} Q_{kj}$ , where for simplicity we have neglected the Eriksen stress, and an active contribution,  $\sigma_{ij}^a = \alpha_2 c^2 Q_{ij}$ , which describes contractile or extensile stresses exerted by the active particles in the direction of the director field. In addition, activity yields a curvature-induced current  $\mathbf{j}^a = -\alpha_1 c^2 \nabla \cdot \mathbf{Q}$  in Eq. (1a) that drives units from regions populated by fast-moving particles to regions of slow-moving particles. The  $c^2$  dependence of the active stress and current is appropriate for systems where activity arises from pair interactions among the filaments via cross-linking motor proteins. The sign of  $\alpha_2$  depends on whether the active particles generate contractile or extensile stresses, with  $\alpha_2 > 0$  for the contractile case and  $\alpha_2 < 0$  for extensile systems, while we assume  $\alpha_1 > 0$ .

To study the dynamics of defects, we consider a pair of opposite-sign half-integer disclinations separated by a distance  $x = x_+ - x_-$ , where  $x_{\pm}$  is the  $x$  coordinate of the  $\pm 1/2$  disclination, respectively, as shown in Figs. 1(a) and 1(b). When backflow is neglected, the pair dynamics is purely relaxational and is controlled by the balance of the attractive force between defects  $\mathbf{F}_{\text{pair}} = -\nabla E_{\text{pair}}$ , with  $E_{\text{pair}} \sim K \log(x/a)$  the energy of a defect pair (with  $a$  the core radius), and an effective frictional force  $\mathbf{F}_{\text{fric}} = \mu \dot{\mathbf{x}}$ , with  $\mu \sim \gamma$  a friction coefficient. Thus  $\mu \dot{\mathbf{x}} = K/x$  and the distance between the annihilating defects decreases according to a square-root law,  $x(t) \propto \sqrt{t_a - t}$ , with  $t_a$  the annihilation time. More precise calculations have shown that the effective friction is itself a function of the defect separation [29, 30],  $\mu = \mu_0 \log(x/a)$ , although this does not imply substantial changes in the overall picture. This simple model predicts that the defect and antidefect approach each other along symmetric trajectories.

We have integrated numerically Eqs. (1) for an initial configuration of uniform concentration and zero flow velocity, with two disclinations of charge  $\pm 1/2$  located on the  $x$  axis of a square  $L \times L$  box at initial positions  $\mathbf{x}_{\pm}(0) = (\pm L/4, 0)$ . The integration is performed using the finite differences scheme described in Ref. [11, 12]. To render Eqs. (1) dimensionless, we normalize distance by the approximate length of the active rods  $\ell = 1/\sqrt{c^*}$ , stress by the elastic stress of the nematic phase  $\sigma = K\ell^{-2}$  and time by  $\tau = \eta\ell^2/K$  representing the ratio between viscous and elastic stress. In these dimensionless units, for simplicity, we let  $\alpha_2 = \alpha$  and take  $\alpha_1 = |\alpha_2|/2$ . Periodic boundary conditions are assumed, and the defects are allowed to evolve until they annihilate. Figure 1 shows a snapshot of the order parameter and flow field shortly after the beginning of the relaxation for both a contractile and extensile system, with  $\alpha = \pm 0.2$  in the units defined above (see also the supplementary movie S1 [31]).

In passive nematic liquid crystals (i.e.,  $\alpha = 0$ ) it is

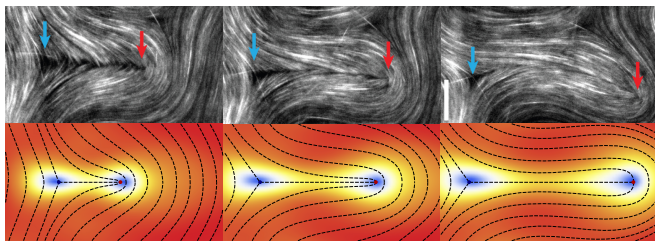


FIG. 2: (color online) Defect pair production in an active suspension of microtubules and kinesin (top) and the same phenomenon observed in our numerical simulation of an extensile nematic fluid with  $\gamma = 100$  and  $\alpha = -0.5$ . The experimental picture is reprinted by permission from T. Sanchez et al., Nature (London) 491, 431 (2012). Copyright 2012, Macmillan.

well known that the dynamics of defects is greatly modified by the so-called backflow, that is, the flow induced by reorientation of the nematic order parameter through the elastic stresses  $\sigma_{ij}^r$  in the Navier-Stokes equation. In particular, when backflow is neglected, the defect and antidefect are predicted to move at the same velocity toward each other until annihilation. Backflow tends to speed up the  $+1/2$  defect and to slow down the  $-1/2$  defect, yielding asymmetric trajectories [25]. In active liquid crystals, the active stress in the Navier-Stokes equation provides a new source for flow associated with inhomogeneities in the order parameter, as demonstrated first in a one-dimensional thin film geometry where activity drives a transition to a spontaneously flowing state [2]. This new *active backflow* can greatly exceed the curvature-driven backflow present in passive systems. Furthermore, the direction of the active backflow is controlled by the sign of the activity parameter  $\alpha$  and, for a given director configuration, has opposite directions in contractile and extensile systems. Backflow arising from active stresses drives the  $+1/2$  defect to move in the direction of its “tail” in contractile systems ( $\alpha > 0$ ) and in the direction of its “head” in extensile systems ( $\alpha < 0$ ), where the terminology arises from the cometlike shape of  $+1/2$  defects. In contrast, due to symmetry considerations, the active backflow vanishes at the core of a  $-1/2$  defect which thus remains stationary under the action of active stresses. We note that active curvature currents in the concentration equation controlled by  $\alpha_1$  have a similar effect, as first noted by Narayan, Ramaswamy, and Menon and collaborators in a system of vibrated granular rods [7]. Such active curvature currents control dynamics in systems with no momentum conservation but are very small here, where the concentration variations remain small, as seen from Figs. 1(c) and 1(d), and flow controls the dynamics.

In contractile systems active backflow yields a net speed-up of the  $+1/2$  defect towards its antidefect for the annihilation shown in Fig. 1(b). In extensile systems, with  $\alpha < 0$ , backflow drives the  $+1/2$  defect to

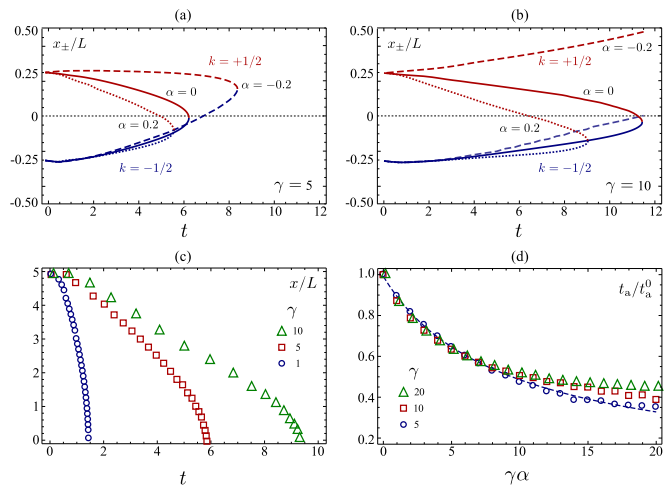


FIG. 3: (color online) Defect trajectories and annihilation times obtained from a numerical integration of Eqs. (1) for various  $\gamma$  and  $\alpha$  values. (a) Defect trajectories for  $\gamma = 5$  and various  $\alpha$  values (indicated in the plot). The upper (red) and lower (blue) curves correspond to the positive and negative disclination, respectively. The defects annihilate where the two curves merge. (b) The same plot for  $\gamma = 10$ . Slowing down the relaxational dynamics of the nematic phase increases the annihilation time and for  $\alpha = -0.2$  reverses the direction of motion of the  $+1/2$  disclination. (c) Defect separation as a function of time for  $\alpha = 0.2$  and various  $\gamma$  values. (d) Annihilation time normalized by the corresponding annihilation time obtained at  $\alpha = 0$  (i.e.,  $t_a^0$ ). The line is a fit to the model described in the text.

move towards its head, away from its  $-1/2$  partner in the configuration of Fig. 1(b), acting like an effectively *repulsive* interaction. This somewhat counterintuitive effect has been observed in experiments with extensile microtubules and kinesin assemblies [16] and can be understood on the basis of the hydrodynamic approach embodied in Eqs. (1). In Fig. 2 we have reproduced from Ref. [16] a sequence of snapshots showing a pair of  $\pm 1/2$  disclinations moving apart from each other together with the same behavior observed in our simulations.

To quantify the dynamics we have reconstructed the trajectories of the defects by tracking the drop in the magnitude of the order parameter. The trajectories are shown in Figs. 3(a) and 3(b), where red lines in the upper portion of the plots represent the trajectory of the  $+1/2$  disclination, while the blue lines in the lower portion of the plot are the trajectories of the  $-1/2$  defect. The tracks end when the cores of the two defects merge. For small activity and small values of the rotational friction  $\gamma$ , the trajectories resemble those obtained in Ref. [25] for passive systems. At large values of activity, however, the asymmetry in defect dynamics becomes more pronounced, and when the activity dominates over orientational relaxation, the  $+1/2$  disclination moves independently along its symmetry axis with a velocity  $\mathbf{v} \propto -\alpha \hat{\mathbf{x}}$ , whose direction is dictated by the sign of  $\alpha$ . This be-

havior is clearly visible in Fig. 3(c), showing the defect separation  $x(t)$  as a function of time. For  $\gamma$  sufficiently large, the trajectories are characterized by two regimes. For large separation the dynamics is dominated by the active backflow, and thus  $\dot{x}(t) \propto -\alpha$  and  $x(t) \propto -\alpha t$ . Once the defects are about to annihilate, the attractive force  $F_{\text{pair}} \propto 1/x$  takes over, and the defects behave as in the passive case with  $x(t) \propto \sqrt{t_a - t}$ .

Building on these results, we now propose a phenomenological one-dimensional model that captures qualitatively the dynamics of pair annihilation in active nematics. By neglecting for simplicity the position dependence of the friction, which we assume constant, the dynamics of a pair of disclinations initially at a distance  $x_0$  along the  $x$  axis is governed by the equations

$$\mu [\dot{x}_{\pm} - v_b(x_{\pm})] = \mp \frac{K}{x_+ - x_-}, \quad (3)$$

where  $v_b(x_{\pm})$  is the backflow field at the position  $x_{\pm}$  of the  $\pm 1/2$  defect, given by  $v_b(x) = v_+(x - x_+) + v_-(x - x_-)$ , with  $v_{\pm}(x)$  the flow field due to an isolated  $\pm 1/2$  defect. We retain only the active contribution to the backflow and replace the flow profiles by their constant values at the core of the defect, with  $v_b(x_+) = v_{\alpha} \propto -\alpha$  and  $v_b(x_-) = 0$ . Note that  $v_{\alpha} < 0$  for contractile systems and  $v_{\alpha} > 0$  for extensile ones. This yields the following simple equation for the pair separation  $\dot{x} = v_{\alpha} - \frac{2\kappa}{x}$ , with  $\kappa = K/\mu$ . This equation explicitly captures the two regimes shown in Fig. 3(c) and described earlier. The solution takes the form

$$x(t) = x_0 + v_{\alpha}t - 2(\kappa/v_{\alpha}) \ln \left[ \frac{x(t) - 2\kappa/v_{\alpha}}{x_0 - 2\kappa/v_{\alpha}} \right]. \quad (4)$$

The pair annihilation time  $t_a$  is determined by  $x(t_a) = 0$  and is given by  $t_a = -x_0/v_{\alpha} - (2\kappa/v_{\alpha}^2) \ln [1 - (x_0 v_{\alpha}/2\kappa)]$ . For passive systems ( $\alpha = 0$ ) this reduces to  $t_a^0 = x_0^2/4\kappa$ . In contractile systems, activity speeds up pair annihilation, while it slows it down in extensile systems. Our simple model predicts that the annihilation time, normalized to its value in passive systems,  $t_a/t_a^0$ , depends only on  $v_{\alpha}x_0/2\kappa \sim \alpha\gamma$ . Figure 3(d) shows a fit of the annihilation times extracted from the numerics to this simple formula. The model qualitatively captures the numerical behavior.

While the effect of activity on the precollisional dynamics of a disclination pair can be accounted for relatively simply in terms of active backflow, the postcollisional behavior is dramatically affected by activity [32]. Figure 4 shows the evolution of the system after annihilation of the initial defect pair (see also the supplementary movie S2 [31]). The frame in Fig. 4(a) shows the initial configuration of the two defects, while Fig. 4(b) shows the configuration just after pair annihilation. The other frames display the evolution in time (with time increasing from left to right and top to bottom). Immediately after collision,

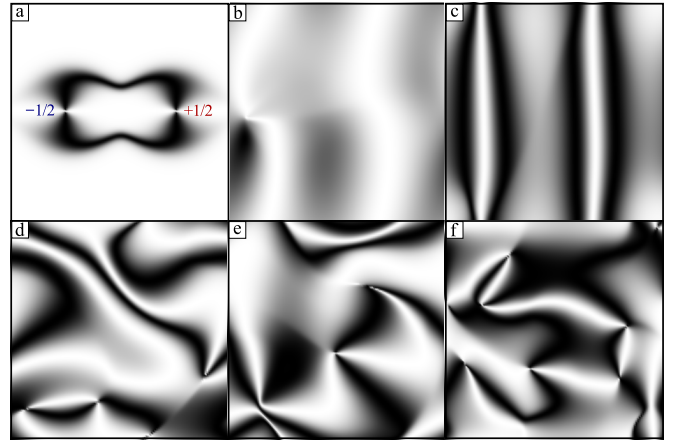


FIG. 4: (color online) Schlieren texture highlighting the post-collisional dynamics of a  $\pm 1/2$  pair for  $\gamma = 10^3$  and  $\alpha = 0.2$ . (a) indicates the initial configuration of the defects, and (b) shows the system immediately after defect annihilation.

the system develops two density or flow bands reminiscent of those observed in the absence of defects [12]. The bands, however, are unstable and quickly start deforming while new defect pairs “pinch off”. The dynamics quickly becomes chaotic, with frequent defect formation and annihilation events in the background of an overall proliferation of defects. The passage of defects through a region of space lowers the local nematic order parameter in that region. At large friction  $\gamma$ , the slow relaxation prevents the restoration of the order parameter to its initial value, leading to a progressive reduction of the average order parameter in time. Complex textures in active nematics were also reported in Ref. [10], although those structures are not easily decomposed in terms of disclinations. More work is needed to fully explore this rich and complex dynamics and formulate a quantitative classification of the behavior of defects in active liquid crystals.

We thank Zvonimir Dogic and Tim Sanchez for several illuminating discussions. L.G. was supported by SISSA mathLab. M.C.M. was supported by the National Science Foundation through Grants No. DMR-1004789 and No. DGE-1068780. M.J.B. and X.M. were supported by the National Science Foundation through Grant No. DMR-0808812 and by funds from the Soft Matter Program of Syracuse University.

- 
- [1] M. C. Marchetti, J. F. Joanny, S. R. Ramaswamy, T. B. Liverpool, J. Prost, M. Rao, and R. A. Simha, arXiv:11207.2929 [Rev. Mod. Phys. (to be published)].
  - [2] R. Voituriez, J. F. Joanny and J. Prost, Europhys. Lett. **70**, 118102 (2005).
  - [3] D. Marenduzzo, E. Orlandini, M. E. Cates, and J. M. Yeomans, Phys. Rev. E **76**, 031921 (2007).

- [4] L. Giomi, M. C. Marchetti and T. B. Liverpool, Phys. Rev. Lett. **101**, 198101 (2008).
- [5] S. Ramaswamy, R. A. Simha and J. Toner, Europhys. Lett. **62**, 196 (2003).
- [6] S. Mishra and S. Ramaswamy, Phys. Rev. Lett. **97**, 090602 (2006).
- [7] V. Narayan, S. Ramaswamy, and N. Menon, Science **317**, **105** (2007).
- [8] A. Sokolov and I. S. Aranson, Phys. Rev. Lett. **103**, 148101 (2009).
- [9] L. Giomi, T. B. Liverpool and M. C. Marchetti, Phys. Rev. E **81**, 051908 (2010).
- [10] S. M. Fielding, D. Marenduzzo, and M. E. Cates, Phys. Rev. E **83**, 041910 (2011).
- [11] L. Giomi, L. Mahadevan, B. Chakraborty, and M. F. Hagan, Phys. Rev. Lett. **106**, 218101 (2011).
- [12] L. Giomi, L. Mahadevan, B. Chakraborty, and M. F. Hagan, Nonlinearity **25**, 2245 (2012).
- [13] H. H. Wensink, J. Dunkel, S. Heidenreich, K. Drescher, R. E. Goldstein, H. Löwen, and J. M. Yeomans, Proc. Natl. Acad. Sci. USA **109**, 14308 (2012).
- [14] M. Kleman and O. Lavrentovich, *Soft Matter Physics: An Introduction* (Springer, New York, 2003).
- [15] R. Kemkemer, D. Kling, D. Kaufmann, and H. H. Gruler, Eur. Phys. J. E **1**, 215 (2000).
- [16] T. Sanchez, D. N. Chen, S. J. DeCamp, M. Heymann, and Z. Dogic, Nature (London) **491**, 431 (2012).
- [17] K. Kruse, J. F. Joanny, F. Jülicher, J. Prost, and K. Sekimoto, Phys. Rev. Lett. **92**, 078101 (2004).
- [18] K. Kruse and F. J. Jülicher, Eur. Phys. J. E **20**, 459 (2006).
- [19] R. Voituriez, J. F. Joanny, and J. Prost, Phys. Rev. Lett. **96**, 028102 (2006).
- [20] J. Elgeti, M. E. Cates, and D. Marenduzzo, Soft Matter **7**, 3177 (2011).
- [21] P. G. de Gennes and J. Prost, *The Physics of Liquid Crystals* (Clarendon, Oxford, 1993).
- [22] M.C. Marchetti, Nature (London) **491**, 340 (2012).
- [23] The approximation of a two-dimensional system is justified in the experiments reported in [16] where the tracking of individual filaments does not show microtubules hopping over each other (Z. Dogic, private communication).
- [24] C. Denniston, Phys. Rev. B **54**, 6272 (1996).
- [25] G. Tóth, C. Denniston, and J. M. Yeomans, Phys. Rev. Lett. **88**, 105504 (2002).
- [26] E. I. Kats, V. V. Lebedev, and S. V. Malinin, J. Exp. Theor. Phys. **95**, 714 (2002).
- [27] D. Svenšek and S. Žumer, Phys. Rev. E **66**, 021712 (2002).
- [28] A. M. Sonnet and E. G. Virga, Liq. Cryst. **36**, 1185 (2009).
- [29] H. Pleiner, Phys. Rev. A **37**, 3986 (1988).
- [30] G. Ryskin and M. Kremenetsky, Phys. Rev. Lett. **67**, 1574 (1991).
- [31] See supplemental Material at <http://link.aps.org/supplemental/10.1103/PhysRevLett.110.228101> for movies of disclination dynamics.
- [32] S. P. Thampi, R. Golestanian and J. M. Yeomans, arXiv:1302.6732 (2013).